

AD/A-004 883

BASIC AND APPLIED RESEARCH IN MATERIALS

J. Bruce Wagner, Jr.

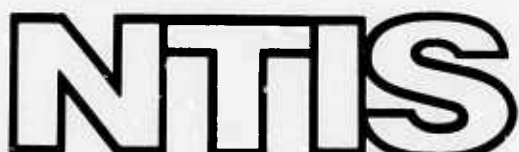
Northwestern University

Prepared for:

Defense Advanced Research Projects Agency

31 May 1974

DISTRIBUTED BY:



National Technical Information Service  
U. S. DEPARTMENT OF COMMERCE

ADA004883

055170

ANNUAL TECHNICAL REPORT

1 June 1973 - 31 May 1974

Sponsored by

Defense Advanced Research Projects Agency

ARPA Order No. 2379

Program Code Number : 3D10

Grantee: Northwestern University

Effective Date of Grant: June 1, 1973

Grant Expiration Date: May 31, 1974

Amount of Grant: \$300,000

Grant Number: DAHC 15 73 G-19

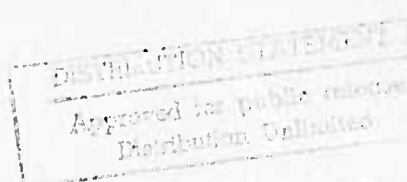
Principal Investigator: J. Bruce Wagner, Jr.

Phone: (312) 492-3606

Title: Basic and Applied Research in Materials



Materials Research Center  
Northwestern University  
Evanston, Illinois 60201



The views and conclusions contained in this document are those of the authors and should not be interpreted as necessarily representing the official policies, either expressed or implied, of the Advanced Research Projects Agency or the U. S. Government.

Reproduced by  
NATIONAL TECHNICAL  
INFORMATION SERVICE  
U.S. Department of Commerce  
Springfield VA 22151

## I. SUMMARY

This report covers the period from 1 June 1973 through 31 May 1974 and describes the research carried out in four major areas: 1) Materials for Energy Storage, 2) Heterogeneous Catalysis, 3) Maximization of Electret Effect in Polyacrylonitrile Films and 4) Properties of Foils Containing Very Short Wavelength Composition Modulations.

### A. Technical Problem and Approach

#### 1. Materials for Energy Storage

The discovery of new types of solid electrolytes (such as beta alumina,  $\text{RbAg}_4\text{I}_6$ , copper and silver halides and stabilized zirconia) with large values of ionic conductivity at relatively low temperatures has enhanced the prospect of developing battery systems possessing a high energy storage-to-weight ratio, high power output capability, long life in service, efficiency in charge-discharge characteristics and the capability of being constructed from inexpensive, readily obtainable materials. Two complementary areas of research are being pursued. The first involves a search for new materials to be used as solid state electrolytes and electrodes, and the second involves detailed studies on electrolytes already known to be predominantly ionic conductors. Toward these ends, studies already underway of cuprous halides as model systems are being continued. Research has been initiated on materials (e.g.,  $\beta$  and  $\beta''$  alumina, some tungsten bronze phases, calcia stabilized zirconia and some hollandites) which can be used over a wider range of operating conditions. Materials of interest will be prepared by sintering as well as by standard crystal growth techniques. Mossbauer and NMR techniques as well as electrical conductivity and dielectric loss properties are being used to characterize these materials.

#### 2. Heterogeneous Catalysis

A number of the most important heterogeneous catalysts consist of tiny crystallites of metal supported on carriers such as alumina or silica. Yet relatively little is known of the effect of particle size and morphology and of the effect of the support upon the catalytic activity. Standard

batches of catalysts are being prepared by different methods, of varying particle sizes and on different supports. These catalysts will be characterized as completely as possible using x-ray photoelectron spectroscopy (to gain information about the surfaces, i.e., support, catalyst etc.), EPR studies (to yield information about the identity of sites at the surface and their electronic nature), kinetic studies (to determine the kinetic form and rate constants for reactions chosen to give optimum information about catalytic characteristics) and selectivity studies (to determine relative yields of several concurrent reactions). When these data have been assembled, an attempt will be made to systematize the results phenomenologically and to develop a theoretical understanding of the underlying phenomenon.

### 3. Maximization of Electret Effect in Polyacrylonitrile Films

Dielectric solids possessing a permanent electric field (electrets) can potentially be used as active elements in a number of devices, e.g., acoustical transducers, infrared detectors, piezoelectric devices and optical second harmonic generators. Polymeric solids make superior electrets because of their thermal and mechanical stability, long chain macromolecular nature (which afford an additional means of orienting dipolar groups) and low cost. These properties will be exploited in the creation of new materials for use in apparatus utilizing the electret effect.

The purpose of the present research is to maximize the electret-related behavior of polyacrylonitrile film using selective modification of physical and chemical microstructures and to gain an understanding of the effect of morphology on the electret effect in polymer solids in general. Initial research is directed toward determining relationships between physical modifications and the magnitude of their effect on the electret effect in polyacrylonitrile. Samples will be prepared both by solution casting and by heating to temperatures above the glassy transition and then cooling in the presence of an electric field. The magnitude of the electret effect produced will be measured and the molecular organization characterized.

### 4. Properties of Foils Containing Very Short Wavelength Composition Modulations

Copper-nickel foils containing very short wavelength (7-60 Å) composition modulations exhibit a surprising increase in ultimate strength

and elastic modulus as the wavelength of the modulation is decreased. There appear to be no theories that account for this increase. The present research is directed toward investigating systems other than Cu-Ni to determine whether the effect is limited to this material and, if not, to develop systems which exhibit even higher elastic moduli. Attempts will be made to extend the range of wavelengths downward from the present 14 Å to 7 Å (which is the smallest wavelength composition attainable with the present setup). A further objective is the fabrication of small components of intricate shape having high strength to weight ratios. Preliminary electrical and magnetic measurements will also be undertaken.

#### B. Technical Results

##### 1. Materials for Energy Storage

Research was conducted on three related systems. These are materials for electrodes, materials for electrolytes in fuel cells and materials for electrolytes in solid state batteries. The work on electrode materials for battery applications has been on two classes of materials, namely, the alkali hollandite phases and the tungsten bronzes. Both these materials exhibit good electronic conduction and can be prepared with a wide range of stoichiometry.

The alkali (K, Rb, Cs) hollandite phases have been prepared by reduction of an alkali titanate, and the diffusion of  $\text{Na}^+$  is being studied using NMR line narrowing-techniques. The tungsten bronzes (general formula  $\text{M}_x\text{WO}_3$ , where M is usually a monovalent cation and x varies between 0 and 1) are also under investigation. Single crystals of  $\text{Na}_x\text{WO}_3$  have successfully been prepared by electrolysis, and the thermodynamic activities of the sodium have been determined on these crystals using a galvanic cell technique. Both of these systems are potentially useful electrode materials.

The research on electrolytes for fuel cells involves studies of a relatively new type electrolyte,  $7\text{Bi}_2\text{O}_3 \cdot 2\text{WO}_3$ . This material was synthesized from bismuth nitrate and tungstic acid. The powders were pressed and sintered and the resulting composition identified by x-ray diffraction. The oxygen ion conductivity of this material has been reported to be an order of magnitude

higher than that of calcia stabilized zirconia, and work is continuing on preparation techniques for different stoichiometries prior to carrying out transport measurements.

The classical oxygen ion electrolyte, calcia stabilized zirconia, has been studied extensively, but there have been questions raised concerning the effect of oxygen leaking via the gas phase from one electrode to the other. Accordingly, the partial conductivities of electrons and electron holes have been redetermined under experimental conditions which blocked such oxygen gas transport. The partial conductivities exhibited a dependence on oxygen pressure of  $\pm 1/4$  as predicted by theory.

The cuprous halides have been used as electrolytes in batteries. However, the reason for the high conductivity due to the  $\text{Cu}^+$  ion has not been ascertained although such information would be of tremendous help in choosing other electrolytes. Accordingly, neutron diffraction techniques have been used to obtain the cation radial pair density function in  $\gamma\text{-CuCl}$ . The observed structure may be explained by a dynamic vibrational mode by which  $\text{Cu}^+$  moves to the faces of the surrounding tetrahedron of  $\text{Cl}^-$ . At the same time the  $\text{Cu}^+ - \text{Cu}^+$  nearest neighbor distance remains fixed. These studies are continuing, and results will be compared to transport properties of  $\text{CuCl}$  already carried out under ARPA support. In a related study, the ionic and electronic conductivities of cuprous iodide have been determined. Results indicate that the transport number of electron holes is  $\approx 10^{-3}$  and that copper (transport number of almost unity) migrates by more than one mechanism as the temperature is changed.

The  $\beta$  and  $\beta''$  aluminas have assumed tremendous importance in present day technology. Crystals have been obtained primarily from industrial companies whose interests lay in refractories and not pure electrolytes. Accordingly, a method for preparation of ultra pure  $\beta$  alumina was successfully tested. The advantages of this method are twofold--high purity and the ability to control the sodium content.

Discs of  $\beta''$  alumina were also prepared by compacting and sintering. The total electrical conductivity of this synthesized electrolyte has been measured, and compatible electrode materials are being sought. In another

project involving the synthesis of new electrolytes, BaO and  $TiO_2$  have been fused to form a hollandite phase now being studied. In addition, other hollandites are being prepared by sintering and by crystal growth in a hollow cathode furnace. These exploratory studies are providing valuable information on the synthesis and preparation of new electrolytes of known composition.

## 2. Heterogeneous Catalysis

Eight batches of platinum on silica have been produced during the report period. They were prepared by two different methods, in sintered and unsintered form and of two mesh sizes. The dispersion was then measured for each catalyst utilizing hydrogen chemisorption in an apparatus constructed especially for this project. These measurements will be verified by two independent industrial laboratories. The electron paramagnetic resonance spectra of  $Pt/SiO_2$  was studied in order to obtain information on the effect of particle size. The results show a definite effect of the support. A special sample holder has been constructed for x-ray measurements of the surface area. The system has been checked out with activated charcoal, and the measurement and data processing steps automated. Measurements on the silica gel support have begun.

An apparatus to study the isotopic exchange between cyclopentane and deuterium has been constructed. This reaction is sensitive to the size and structure of the metal particles. A flow reactor has also been constructed and put into operation to study a reaction that is insensitive to structure, namely, the hydrogenolysis of cyclopropane. Using this reactor, the activity of one of the catalysts was determined from  $-12^\circ C$  to  $22^\circ C$ . The turnover number and activation energy were also determined. Similar measurements are currently being made on the other three  $Pt/SiO_2$  catalysts in the series.

## 3. Maximization of Electret Effect in Polyacrylonitrile Films

Permanent electrical polarization in PAN films is due to at least four sources, whose relaxations can be observed in TSD curves as  $\alpha$ ,  $\beta$ ,  $\gamma$  and  $\delta$  peaks. The  $\beta$  peak is thought to be associated with partial loss of preferred orientation of dipoles in paracrystalline domains, while the  $\alpha$  peak appears to originate from disorientation of dipoles in amorphous regions.

This  $\alpha$  peak is two orders of magnitude stronger than the  $\beta$  peak and suggests, therefore, that polarization within PAN resides largely in disordered regions. It appears, also, that this polarization is due to fairly extensive structures involving large numbers of individual dipoles. This proposition is supported by such observations as 1) the enhancement of birefringence due to polarization across the thickness of these films is uniform, 2) the activation energy of the  $\alpha$  relaxation is sufficiently large that cooperative motions about several interatomic bonds must be considered as the elemental mechanism in its depolarization, and 3) its polarization can be reversed in sign even by poling at temperatures substantially below those at which this polarization will relax to zero. Note: This "switching" effect might be a very useful property for exploitation in future electronic devices. Furthermore, the fact that no change in interatomic packing can be detected in polarized films might actually be evidence for a polarization domain structure. This would mean that unpolarized films would have domains whose orientations and mass fractions are such that there may or may not be a measurable bulk polarization, but application of an external electric field would bias these orientations and amounts to giving the resulting levels a residual polarization. Thus, PAN need not acquire a new kind of interatomic packing; rather, the material would simply have to adjust its domains to exhibit a permanent electrical polarization. More work both of an experimental and theoretical nature needs to be done to explore these possibilities.

#### 4. Mechanical Properties of Composition Modulated Foils

Extensive numerical calculations have been carried out to obtain the proper expression for the strain generated in a "bulged" foil, and an exact solution has been obtained. The correction required to allow for the strong  $\langle 111 \rangle$  texture in the samples has also been calculated. These results have been utilized to analyze data obtained in a closely related study of Cu-Ni foils. Several attempts to evaporate Cu-Pd modulated foils have been unsuccessful. This project will therefore be phased out of the current program.

## II. RESEARCH REPORTS

### A. Materials for Energy Storage

#### Faculty:

D. H. Whitmore, Professor, Materials Science, Group Leader  
D. L. Johnson, Professor, Materials Science  
L. H. Schwartz, Professor, Materials Science  
J. B. Wagner, Professor, Materials Science  
L. B. Welsh, Assistant Professor, Physics

#### Research Staff:

W. Jakubowski, Visiting Scholar  
H. M. Lee, Postdoctoral Research Associate  
P. Raychaudhuri, Postdoctoral Fellow  
W. A. Spurgeon, Visiting Scholar  
T. Wada, Visiting Scholar  
W. Wahnsiedler, Visiting Scholar

#### Graduate Students:

D. Bouchon  
D. Girard  
T. Jow  
B. J. Mueller  
J. Schreurs

#### 1. Electrolyte Materials for Fuel Cell Applications

##### a. Transport Measurements in Ca-Stabilized $ZrO_2$ at Elevated Temperatures

In an earlier investigation by Patterson et al (A1) of partial conductivities of Ca-stabilized  $ZrO_2$  utilizing a d-c polarization technique, a blocking electrode was coated on one side of the electrolyte sample and a reversible electrode (various equilibrium metal/oxide mixtures) was placed in contact with the opposite side. Heyne (A2) objected to such a cell configuration on the basis that an interfering process may take place at the free

sides of the sample (those on which no blocking electrode material was present to close off the surrounding gas), thereby disturbing the uniformity of the gradients inside the sample through the exchange of oxygen with the surrounding gas atmosphere. If this were to occur, Heyne argues that the partial current observed in the final stationary state may not depend solely on the applied voltage but also on the oxygen exchange rate at the free surfaces of the electrolyte sample.

Because of the aforementioned possibility occurring in the experiments of Patterson et al (A1) which casts some doubt on their findings, studies were undertaken to redetermine the partial conductivities of holes ( $\sigma_{\oplus}$ ) and electrons ( $\sigma_{\ominus}$ ) in Ca-stabilized  $ZrO_2$  using a dc polarization cell in which precautions were taken to coat all the surfaces but one with the blocking electrode material (Pt) to prevent oxygen exchange between the electrolyte and the gas phase. Towards that end, all surfaces of the electrolyte sample except one were coated with platinum paste and then fired at  $1000^{\circ}C$  for several hours. To insure a nonporous electrode coating on these surfaces, the procedure was repeated, and finally a Pt cup was positioned over them and the sample fired again to accomplish a strong and nonporous bond between the Pt paste and the cup.

Initially, metal/metal oxide mixture electrodes were employed as the reversible electrodes for the cell, contact was made between this electrode and the uncoated surface of the electrolyte sample and the sample was heated to temperatures in the range  $900^{\circ}$  to  $1200^{\circ}C$  in a stream of purified argon. The partial conductivity results, so obtained, were in good agreement with those of Patterson et al. Next, the same polarization cell, but without the metal/metal oxide electrode, was placed in a stream of metered  $CO/CO_2$  gas mixture. With this latter configuration, the  $\mu_{O_2}$  was maintained constant at the bare (uncoated) surface of the electrolyte sample since all of the remaining surfaces were blocked with respect to the surrounding gas phase. The results obtained with the aid of this latter cell were compared with those obtained with the metal/metal oxide reversible electrode, and it was found that the reproducibility of the data was better when relatively thick electrolyte samples were employed.

Analysis and plotting of the polarization data from the present experiments, accomplished by using the Wagner equations and the plotting method outlined by Patterson et al. (A1), yielded  $\sigma_{\oplus}$  and  $\sigma_{\ominus}$  values over the temperature range 900° to 1200°C and a wide range of  $P_{O_2}$ . The partial conductivity results exhibited the usual  $P_{O_2}^{\pm\frac{1}{4}}$  dependence. Combining data for the total conductivity of the electrolyte with that for the partial conductivities allows an estimation to be made of the range of  $P_{O_2}$  for satisfactory operation of Ca-stabilized  $ZrO_2$  as a solid electrolyte at temperatures from 900° to 1200°C.

b. Study of the Sintering Characteristics of the Compound  
 $7Bi_2O_3 \cdot 2WO_3$

It was recently reported by Takahaski and Iwahara (A3) that the ionic compound  $7Bi_2O_3 \cdot 2WO_3$  exhibited an oxygen ion conductivity at least an order of magnitude higher than that of the widely-known oxygen ion conductor, stabilized zirconia. This compound was synthesized at Northwestern by calcining bismuth nitrate at 700°C for two hours to convert it to the oxide, milling it with tungstic acid and calcining the resulting mixture for ten hours at 750°C. X-ray diffraction powder patterns indicated that the powder, so prepared, was the desired phase. Cold pressing this powder at 25,000 psi in an isostatic press yielded a compact with 67% density.

An organic precursor approach is also being investigated for preparation of highly sinterable chemically homogeneous powders. This method was originally developed to produce  $BaTiO_3$  (A4), but can be adapted to many oxide systems. Soluble salts of the cations are dissolved in a solution of citric acid in ethylene glycol. Stoichiometry of mixed oxides can be accurately controlled by preparing separate solutions of each of the cations. After mixing to the proper proportions, the solution is heated to remove excess solvent, resulting in an organic glass containing the metallic ions in solution. This is then calcined at ~ 650°C to decompose the glass and drive off the organic constituents. A fine particle size, highly-sinterable, chemically homogeneous oxide powder results. Sintering temperatures are typically much lower than possible with conventional powders, resulting in less loss of volatile constituents.

## 2. Electrolyte Materials for Battery Applications

### a. Structure Study of the Solid Electrolyte $\gamma$ -CuCl

The cation radial pair density function has been studied to gain insight into the mechanism governing the high cationic mobility in CuCl, taken here as a prototype for halide ionic conductors. Three samples of  $\gamma$ -CuCl ( $F\bar{4}3m$ ) have been prepared with different isotopic composition of the Cu-component: 99.7% Cu-63, natural Cu, and 99.7% Cu-65. Powder neutron diffraction patterns were taken at 25°C and at 366°C up to  $\sin \theta/\lambda = 0.8 \text{ \AA}^{-1}$ . The Fourier Transform of the coherent differential scattering cross section curves is a known function of the radial pair density functions for CuCu, CuCl and ClCl. From the positions of the atoms in the unit cell, two temperature factors and a series of coupling factors, one can, with a gaussian broadening, calculate the radial density functions generated by the model (A5). The model at the basis of the fit remains the sphalerite structure. A least squares fitting procedure, with calculated termination error, reveals a striking difference between the CuCu and the ClCl partial densities: the ClCl curves show well resolved density peaks out to large distances while the CuCu-curves exhibit only one main maximum, followed by rapidly damped oscillations about the average density. A comparison between integrated intensity analysis (II) and radial density analysis (RD) shows that the incorporation of the diffuse scattering in the latter affects primarily the temperature factor of the Cu-atom. With  $d = \text{first neighbor distance}$ ,  $\delta = \langle u^2 \rangle^{1/2}/d$  at 25°C is found to be 0.17 for Cu and 0.11 for Cl (II) or 0.26 for Cu and 0.11 for Cl (RD). The values at 366°C are found to be 0.29 and 0.15 (II) or 0.41 and 0.18 (RD). A model calculation shows that the observed structure may be explained by a dynamic vibrational mode which takes Cu ions to the faces of the surrounding tetrahedron of Cl ions, always maintaining the Cu-Cl nearest neighbor separation fixed. The highly correlated nearest neighbor vibration implied by this model is consistent with the low first neighbor coupling parameter obtained when the Kaplow et al analysis (A5) is applied to the data. Studies are continuing to confirm that all the diffuse scattering is indeed inelastic as implied by the model.

b. Electrical Properties of CuI

The cuprous halides are known to be predominantly ionic conductors with the transport number for copper being nearly unity. Very little is known about the behavior of these electrolytes when they are subjected to a bias voltage, especially a transient voltage. In analogy to previous work on cuprous chloride (A6), the electrical properties of CuI have been studied. A symmetrical cell, Cu | CuI | Cu was assembled using 5N cuprous iodide powder which was hydrostatically pressed under 45,000 psi. The resulting compacts were sectioned into right cylinders and sandwiched between two 5N copper electrodes. Using a conventional ac bridge, the total conductivity was measured between 100° and 450°C. When an Arrhenius plot of conductance versus temperature was made, the resultant curve suggests that copper might be migrating by more than one mechanism, i.e., more than one defect may be operative. The calculated conductivities vary from about  $10^{-1} \Omega^{-1} \text{ cm}^{-1}$  at 450° to  $5 \times 10^{-5} \Omega^{-1} \text{ cm}^{-1}$  at 100°C. In order to determine the electronic conductivity (the electronic leakage in a predominantly ionic conductor), an asymmetric cell of the form Cu | CuI | graphite was assembled. The cell was biased by a voltage E which was always much less than the decomposition voltage, the left hand side being the negative pole. Under these conditions, C. Wagner (A7) has shown that the electronic current,  $I_{\text{elec}}$ , under steady state conditions is given by

$$\begin{aligned} I_{\text{elec}} &= I_{\Theta} + I_{\oplus} \\ &= \frac{RTA}{LF} \left\{ \sigma_{\Theta}^{\circ} [1 - \exp(-EF/RT)] \right. \\ &\quad \left. + \sigma_{\oplus}^{\circ} [\exp(EF/RT) - 1] \right\}, \end{aligned}$$

where

- $I_{\Theta}$  = current in amps due to electrons,
- $I_{\oplus}$  = current in amps due to electron holes,
- R = gas constant in joules/eq-deg,
- T = temperature in °K,
- A = cross sectional area of sample in  $\text{cm}^2$
- L = length of sample in cm,
- F = Faraday's constant,

$\sigma_{\Theta}^{\circ}$ ,  $\sigma_{\oplus}^{\circ}$  = conductivity due to electrons and electron holes respectively in MX equilibrated with M

and  $E$  = bias voltage.

Under the conditions of the present experiments,  $\sigma_{\oplus}^{\circ} \gg \sigma_{\Theta}^{\circ}$ ; thus, when  $E \gg F/RT$

$$I_{\text{elec}} = I_{\oplus} = \sigma_{\oplus}^{\circ} [\exp (+ EF/RT)] .$$

The present experiments have shown that at 352°C, a plot of  $\log I_{\oplus}$  versus  $E$  yields a straight line of slope  $F/RT$  in agreement with the above equation. Moreover, the intercept at zero voltage yields a value of  $\sigma_{\oplus}^{\circ} \approx 10^{-4}$ . The total conductivity is given by,

$$\sigma^{\circ} (\text{total}) = \sigma^{\circ} (\text{ionic}) + \sigma^{\circ} (\text{electronic}) = \sigma_i^{\circ} + \sigma_{\oplus}^{\circ} .$$

At temperatures between 350° and 400°C,  $\sigma_i^{\circ} \gg \sigma_{\oplus}^{\circ}$  so that  $\sigma^{\circ} (\text{total}) \approx \sigma_i^{\circ}$ . Therefore, the transport number for electron holes is approximately equal to  $(\sigma^{\circ} (\text{total})/\sigma_{\oplus}^{\circ}) = (10^{-4}/5 \times 10^{-2}) = 2 \times 10^{-3}$ . Thus, CuI may be used as a solid state electrolyte.

At low temperatures plots of  $\log I_{\oplus}$  versus  $E$  are linear, but the theoretical slope of  $F/2.3RT$  is not observed. The slopes are lower than predicted. Moreover, as the voltage is increased (although still below the decomposition voltage), there is an abrupt change in the curve, and the slope decreases. Both these results suggest that electronic leakage becomes more pronounced under these conditions. Studies are underway to clarify this.

When a transient voltage is applied to an electrolyte, three processes may occur. These are (1) redistribution of electronic carriers within the electrolyte, (2) charging or discharging of a double layer capacitance at the electrolyte inert electrode [e.g., CuI | graphite] interface and (3) diffusion of a component into the inert electrode. In the present studies, attention is being directed to items (1) and (2). Inasmuch as copper is virtually insoluble in graphite at these temperatures, diffusion into the graphite can be neglected.

A double cell consisting of CuI samples of differing lengths but of identical cross sectional areas has been assembled. Each sample is sandwiched between copper and graphite. A steady state voltage  $E_1$  is applied to both samples of CuI at the same time. Then the voltage is abruptly changed to a second voltage  $E_2$ . The time to redistribute the electron holes is monitored in each sample. The charge transferred depends on the volume of the samples and, hence, their lengths. On the other hand, the double layer capacitance depends only on the cross sectional area. By using samples of differing lengths, the contribution due to double layer capacitance can be separated from that due to the redistribution of the electronic carriers. A Data General Nova computer has been interfaced with the voltage and current sensing devices, and programs have been written to acquire and process the data. Preliminary data have been obtained on the double layer capacitance, and log I versus time plots appear linear as would be expected from

$$I(t) = I_0 e^{-t/RC},$$

where

$I(t)$  = time dependent electronic current,

$t$  = time,

$R$  = Resistance

and

$C$  = double layer capacitance

Measurements are being continued.

### c. Hollandite Phases Based on $TiO_2$

Work has begun on new materials, based on rutile, which possess the hollandite structure. This structure has two channel sites per formula unit and contains a large concentration of vacancies, with the result that high mobilities for alkali or alkaline earth ions along the channels are expected. Direct fusion of BaO and  $TiO_2$  in our laboratories produced a Ba hollandite phase which was invariably bluish-black in color and was a good electronic conductor due to the presence of Ti ions in two different valence states. However, the electronic component of the electrical conductivity can be suppressed by introducing  $Mg^{2+}$  ions as an isomorphous substitute for  $Ti^{4+}$  ions in the host lattice. The  $Ba_x(Ti_{8-x}Mg_x)O_{16}$  [0.6  $\leq x \leq 1.14$ ]

compounds produced in this manner possess a channel structure formed by a host framework  $(\text{Ti}_{8-x}\text{Mg}_x)\text{O}_{16}$ , with the  $\text{Ba}^{2+}$  ions occupying some of the available lattice sites within the tunnels.

Polycrystalline hollandites were also synthesized from high-purity oxides and carbonates by a solid state reaction at  $1200^\circ\text{C}$  as suggested by Singer et al (A8). Increasing the sintering temperature to  $1400^\circ\text{C}$  yielded black samples possessing relatively high electrical resistivities. These hollandite phases were found to be stable when heated in air to temperatures of  $\sim 900^\circ\text{C}$ .

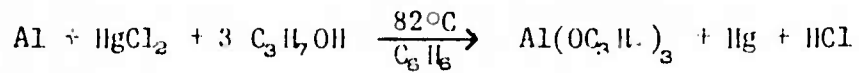
Because the aforementioned Ba hollandite melts incongruently at  $1450^\circ\text{C}$ , it is essential that single crystals of this material be grown in a slightly reducing atmosphere. Attempts are now being made to prepare single crystals of the Ba hollandites using pressed and sintered rods of this phase as the starting material and a hollow cathode-plasma beam-floating zone method. In this method, the two sintered rods are joined through the creation of a molten zone within the hollow cathode, and this narrow molten zone is passed up and down the length of the joined rods by translation of the rod specimen through the cathode, thereby producing a single crystal several inches long. Very preliminary experiments have demonstrated that it is indeed possible to melt a Ba hollandite material with this method, maintain the molten zone for  $> \frac{1}{2}$  hour and pass this zone over a length of a few centimeters.

#### d. Synthesis of Ultra-Pure $\beta$ -Alumina

It is now generally recognized that sodium  $\beta$ -alumina is the best of the presently available electrolyte materials for high-performance, rechargeable battery applications. Yet little is known about the role impurities play in controlling the ionic conductivity in this material. Accordingly, to investigate such effects it seems desirable to first prepare ultra-pure  $\beta$ -alumina and then systematically dope this material with various impurities and determine their influence on the ionic transport properties.

We have elected to prepare ultra-pure  $\beta$ -alumina from the appropriate metal alkoxides by the method developed by Mazdiyasni et al (A9).

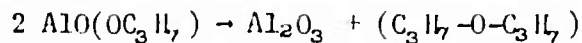
In this method, the aluminum isopropoxide is prepared by the following reaction:



The isopropoxide in benzene is removed under reduced pressure and the product is purified by recrystallization from  $\text{C}_3\text{H}_7\text{OH}$ . The alkoxides react rapidly with traces of water to form alkyl alkoxides according to the reaction:



The alkoxide is then decomposed to the oxide according to the reaction:



All reactions can be carried out in the common solvent benzene. Since sodium (as well as magnesium) also forms an alkoxide, it is possible to mix the aluminum and sodium alkoxides in the right proportions to form  $\text{Na}_2\text{O} \cdot 11 \text{Al}_2\text{O}_3$  ( $\text{Na} \beta$ -alumina).

This method has the following advantages: (1) the mixture can be produced with excellent homogeneity, (2) the mixture, which consists of submicron size powder, can be sintered at unusually low temperatures to yield sodium  $\beta$ -alumina of nearly theoretical density and (3) the hydrous mixture can be fabricated into numerous interesting forms.

e. Measurements of the Total Conductivity of  $\beta''$ -alumina is rhombohedral with space group  $\text{R}\bar{3}\text{m}$  and, except for a  $c$ -axis that is 1.5 times as large, is similar to  $\beta$ -alumina. However, in contrast to  $\beta$ -alumina which has two 11 Å spinel blocks related by a two-fold screw axis parallel to the  $c$ -axis,  $\beta''$ -alumina has three 11 Å spinel blocks related by a three-fold screw axis. As in the case in  $\beta$ -alumina, the spinel blocks are held apart by Al-O-Al bonds, and all of the  $\text{Na}^+$  ions are contained in the planes (the "channels") between the spinel blocks.

Thus,  $\beta''$ -alumina possesses two-dimensional channels partially filled with, e.g., a monovalent cation like  $\text{Na}^+$ , a situation which is likely to lead to exceptionally rapid migration of these cations within the channels at temperatures at or near the ambient. Indeed, preliminary experiments

using Pt electrodes indicate that the ionic resistivity of  $\beta''$ -alumina is lower than that of  $\beta$ -alumina at temperatures ranging from 300° to 800°K.

Because polarization occurs at the Pt electrodes applied to a  $\beta''$ -alumina sample even at frequencies as high as those in the low MHz range, it was decided to measure the conductivity of  $\beta''$ -alumina samples with the aid of electrodes which are reversible both to electrons and the mobile cations in the  $\beta''$ -alumina sample (usually  $\text{Na}^+$  ions in our samples). The reversible electrode material should display a reasonably rapid diffusivity of the cation species in question, possess a high electronic conductivity, be chemically inert towards the sample, have a wide range of nonstoichiometry if it is a compound phase and exhibit all these properties over a wide range of temperatures and partial pressures of the sample's components. Sodium tungsten bronze [ $\text{Na}_x\text{WO}_3$  where  $x \lesssim 0.4$ ] with the tetragonal I structure has been found to be a reversible electrode material when applied to a sodium  $\beta$ -alumina sample (AlO). Because of this finding, polycrystalline samples of the tetragonal  $\text{Na}_x\text{WO}_3$  were synthesized for use as reversible electrodes with sodium  $\beta''$ -alumina by reacting  $\text{Na}_2\text{WO}_4$ ,  $\text{WO}_3$  and W together in the correct proportions.

Discs of sodium  $\beta''$ -alumina were prepared by mixing  $\text{Al}_2\text{O}_3$  powder with  $\text{Na}_2\text{CO}_3$  and small concentrations of  $\text{ZrO}_2$  and  $\text{MgO}$ , compacting and sintering this at 1000°C. The additives  $\text{ZrO}_2$  and  $\text{MgO}$  were found to improve the sinterability of the  $\beta''$ -alumina compact. The total conductivity measurements now underway on such samples employ a Wayne-Kerr ac Universal Bridge and a constant frequency of 1592 Hz. A standard two-probe method was used to measure the conductivity of the sample which was heated in a closed sample chamber through which a stream of purified helium gas flows. Our preliminary results indicate that a thin dielectric layer forms on the surfaces of the sodium  $\beta''$ -alumina sample which have been in contact with the tungsten bronze electrodes; this layer undoubtedly results from a reaction between the electrodes and the sample and undoubtedly gives rise to spurious conductivity results. Accordingly, other reversible electrode materials will be sought.

### 3. Electrode Materials for Battery Applications

#### a. Alkali Hollandite Phases

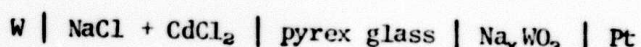
Some alkali hollandite phases (alkali metal = K, Rb, Cs) have been prepared by the reduction of an alkali titanate at 1000°C. The resulting compounds were intensely blue-black in color and possessed the following properties which make them attractive candidates as electrode materials in a high-performance, rechargeable battery system: (1) a wide range of nonstoichiometry so that it can act as both a source and sink of the alkali ions; (2) it exhibits fast transport of the alkali ions; (3) it possesses a high electronic conductivity and (4) it is chemically inert towards most solid electrolytes. We are in the process of evaluating the diffusivity of  $\text{Na}^+$  ions in this material by NMR line-narrowing techniques.

#### b. Thermodynamic Study of Cubic Tungsten Bronze by the EMF Method

The tungsten bronzes are a group of nonstoichiometric compounds that possess the general formula  $\text{M}_x\text{WO}_3$ , where M is usually a monovalent cation and x lies between 0 and 1. These compounds are good electrical conductors, exhibit a variety of structures, and are potential electrode materials for solid-state batteries. Since there is a dearth of thermodynamic data for these materials, an attempt was made here to measure the partial molar thermodynamic properties for Na in  $\text{Na}_x\text{WO}_3$  bronzes employing the EMF method with pyrex glass as the solid electrolyte.

Single crystals of  $\text{Na}_x\text{WO}_3$  samples were prepared by electrolysis of a fused mixture of  $\text{Na}_2\text{WO}_6$  and  $\text{WO}_3$  in an alumina crucible at about 800°C with platinum electrodes. Crystal growth occurred on the cathode, and current densities of about 20 mA/cm<sup>2</sup> yielded the best crystals. Large single crystals were obtained by using a seed crystal over the end of the cathode. A good portion of each crystal was crushed and the bronze powder was used as a sample in the cell described below.

Sodium activities were determined by emf measurements on cells of the type



in which a pyrex glass tube acts as the solid electrolyte. A mixture of

NaCl (40 m/o) and CdCl<sub>2</sub> was employed as the reference electrode since this mixture exhibits ideal mixing behavior. The specimen to be measured was packed in a capillary tube in which a platinum wire had been sealed; in turn, this capillary tube was sealed within a tube of pyrex glass to prevent the loss of sodium during the course of the measurements. The temperature range covered was 400° to 600°C, the cell emf being stable over this range. Above 600°C, the emf fluctuated and the pyrex glass tube swelled due to the fact that the softening point of the glass had been exceeded.

After loading the specimen into the cell, the cell was maintained at 550°C for several days to homogenize the bronze. The open-circuit voltage was measured with the aid of a digital voltmeter. After the measurements, the cell was broken open, and the sample was chemically analyzed for its sodium content. The composition of the sample was determined from x-ray lattice parameter measurements.

The measured emf (E) is given by the relation:

$$E = -\frac{RT}{F} \ln \frac{a'_{\text{Na}}}{a''_{\text{Na}}}$$

where  $a'_{\text{Na}}$  is the activity of sodium in  $\text{Na}_x\text{WO}_3$  and  $a''_{\text{Na}}$  the activity of sodium in NaCl + CdCl<sub>2</sub> mixture. The partial molar entropy, enthalpy and free energy of Na in  $\text{Na}_x\text{WO}_3$  are calculated from standard thermodynamic relationships. The results are shown in Table A-1 below.

The partial molar free energy of Na in the bronze has been observed to be a linear function of temperature over the range 400° to 600°C; accordingly, the partial molar enthalpy and entropy of Na are independent of temperature over this range. Moreover, it has been found that these latter thermodynamic quantities become more negative as the sodium content of the bronze decreases.

TABLE A-1

 Partial Molar Thermodynamic Quantities as a Function of Composition  
 for Cubic Sodium Tungsten Bronzes

Composition	$-\Delta\bar{H}_{\text{Na}}$ (cal/mole)	$-\Delta\bar{S}_{\text{Na}}$ (cal/mole-deg.)
$\text{Na}_{0.8}\text{W}_3$	9,600	21.0
$\text{Na}_{0.7}\text{W}_3$	10,800	21.5
$\text{Na}_{0.4}\text{W}_3$	17,850	28.0

## References

- A- 1. J. W. Patterson, E. C. Bogren and R. A. Rapp, J. Electrochem. Soc. 114, 752 (1967).
- A- 2. L. Heyne in Mass Transport in Oxides, N.B.S. Spec. Publ. 296, Washington, D. C. (1968).
- A- 3. T. Takahashi and H. Iwahara, J. Appl. Electrochem. 3, 65 (1973).
- A- 4. N. Pechini, U.S. Patent No. 3,330,697.
- A- 5. R. Kaplow, B. L. Averbach and S. L. Strong, J. Phys. Chem. Solids 25, 1195 (1964).
- A- 6. J. B. Wagner, Jr., "Electronic Conductivity, Mobility and Double Layer Capacity in Solid State Electrolytes," in Fast Ion Transport in Solids, North Holland Pub. Co. (1973), ed. by W. van Gool.
- A- 7. C. Wagner, International Committee of Electrochemical Thermodynamics and Kinetics, Proc. 7th Meeting (1955), Butterworths, London (1956).
- A- 8. J. Singer, H. E. Kautz, W. L. Fielder and J. S. Fordyce, in Fast Ion Transport in Solids, ed. by W. van Gool (Amsterdam: North-Holland, 1973), p. 653.
- A- 9. K. S. Mazdiyasni, C. T. Lynch and J. S. Smith, J. Am. Ceram. Soc. 48, 372 (1965).
- A-10. M. S. Whittingham and R. A. Huggins, J. Chem. Phys. 54, 414 (1971).

## B. Heterogeneous Catalysis

### Faculty:

R. L. Burwell, Professor, Chemistry, Group Leader  
J. B. Butt, Professor, Chemical Engineering  
J. B. Cohen, Professor, Materials Science  
B. M. Hofiman, Associate Professor, Chemistry  
J. E. Lester, Assistant Professor, Chemistry

### Research Staff:

M. Nestdagh, Postdoctoral Research Associate  
T. Uchijima, Postdoctoral Research Associate  
K. Chung, undergraduate technician

### Graduate Students:

P. H. Schipper  
C. Sorrentino

Supported catalysts, i.e., materials in which a relatively small amount of catalytic ingredient is supported upon a carrier which is usually of large surface area, are widely used industrially. Platinum on silica and platinum on alumina are examples of such catalysts. There is still considerable uncertainty as to the effect of the support and of the particle size of the active ingredient on the catalytic activity. The objective of this project is to contribute to an understanding of these catalysts.

A variety of supported catalysts are to be prepared, characterized by physical techniques, and the results of several reactions upon the catalysts studied. The first objective is to ascertain the effect of the method of preparation of a given catalyst on the catalytic behavior as well as the effect of various particle sizes of the catalytic ingredient. In later work the effect of various supports will be investigated. It is hoped that correlations among all these data will provide some insight into the nature of supported catalysts.

### 1. Catalyst Preparation

The first system investigated was platinum on silica. Davison wide-pore silica gel grade 62 was sieved and then treated with dilute nitric acid, washed and dried. Batches of  $\text{Pt SiO}_2$  were prepared by two different methods and a portion of each batch sintered. Furthermore, catalysts were duplicated--one set on 70-80 mesh silica gel and the other on 120-140. Two mesh sizes of catalysts are needed to determine whether rates are influenced by diffusion. Eight samples of catalyst were thus produced, of two different preparations, both sintered and unsintered and of two mesh sizes.

### 2. Physical Characterization

The catalyst samples were then characterized as thoroughly as possible by physical techniques. Dispersion (the ratio of surface atoms of platinum to the total number of atoms of platinum in %) was first measured by hydrogen chemisorption. This procedure involves the assumption that one hydrogen atom is strongly chemisorbed at  $25^\circ\text{C}$  on the clean catalyst per surface atom. An apparatus was constructed to measure this property. Helium is first used to purge the catalyst of hydrogen. Pulses of hydrogen are then injected which pass over the catalyst and are measured catharometrically. Neon is used as the carrier gas during this stage since helium and hydrogen have nearly the same thermal conductivity. The apparatus gives excellent reproducibility; the dispersions of all of the catalysts have been measured. The results are shown in Table B-1. Since it is essential to know the dispersions as accurately as possible, arrangements have been made for two industrial laboratories to measure independently the dispersion of our samples.

In order to provide information on the effect of particle size, the electron paramagnetic resonance spectra of  $\text{Pt/SiO}_2$  to which a paramagnetic probe molecule had been added was studied. Initial measurements were made using di-*t*-butyl nitroxide as the probe molecule. This effort was unsuccessful because of the strong background from the nitroxide adsorbed on the silica. However, a very interesting effect of the support was found. The nitroxide is very strongly adsorbed by silica, and at coverages below a monolayer, the nitroxide has zero dissociation pressure at  $25^\circ\text{C}$ . If hydrogen

TABLE B-1  
Platinum/Silica Gel Catalysts

Method of Preparation	Mesh of SiO <sub>2</sub>	Identifying Number	Pt Content wt.-%	Dispersion %	Amount in g.
Impregnation with H <sub>2</sub> PtCl <sub>6</sub>	70-80	65	1.10	43.1	300
	120-140	66	1.17	40.7	200
H <sub>2</sub> PtCl <sub>6</sub> , then sintered	70-80	89	1.97	7.1	300
	120-140	88	1.91	7.2	200
Ion exchange with Pt(NH <sub>3</sub> ) <sub>4</sub>	70-80	67	0.49	65.2	300
	120-140	68	0.86	83.5	110
	120-140	87	0.48	80.0	100
Ion exchanged then sintered	70-80	69-1	1.48	22.3	200
	70-80	69-2	1.48	19.7	100
	120-140	70	1.48	28.0	200

is added to Pt/SiO<sub>2</sub> covered with the nitroxide at 25°C, the ESR signal disappears immediately. Even at -78°C, the half-life is only 5-10 min. If the hydrogen is removed after the signal has disappeared and oxygen added at 0°C, the signal of nitroxide returns. Thus, the nitroxide is first reduced to the hydroxylamine and that is then reoxidized to the nitroxide. Since the platinum particles are separated by about 100 Å, diffusion must occur. Since it is unlikely that the platinum particles diffuse at -78°C or that hydrogen atoms diffuse from platinum onto the silica gel, it is postulated that the nitroxide and perhaps the hydroxylamine diffuse on silica relatively rapidly. This work shows a definite effect of the support. These results must be compared with Pt/Al<sub>2</sub>O<sub>3</sub> and others.

X-ray techniques will also be applied to the physical characterization of the catalysts. Toward this end, procedures have been established and tested for measuring the surface area by means of x-rays. A special sample holder which utilizes beryllium windows and is capable of being evacuated and simultaneously heated to 200°C has been constructed. Tests with activated charcoal have given excellent agreement with published data, and a careful study has been made of the error limits. The entire procedure of measurement

and data processing to obtain surface area and particle size has been successfully automated, and measurements on the silica gel support have begun.

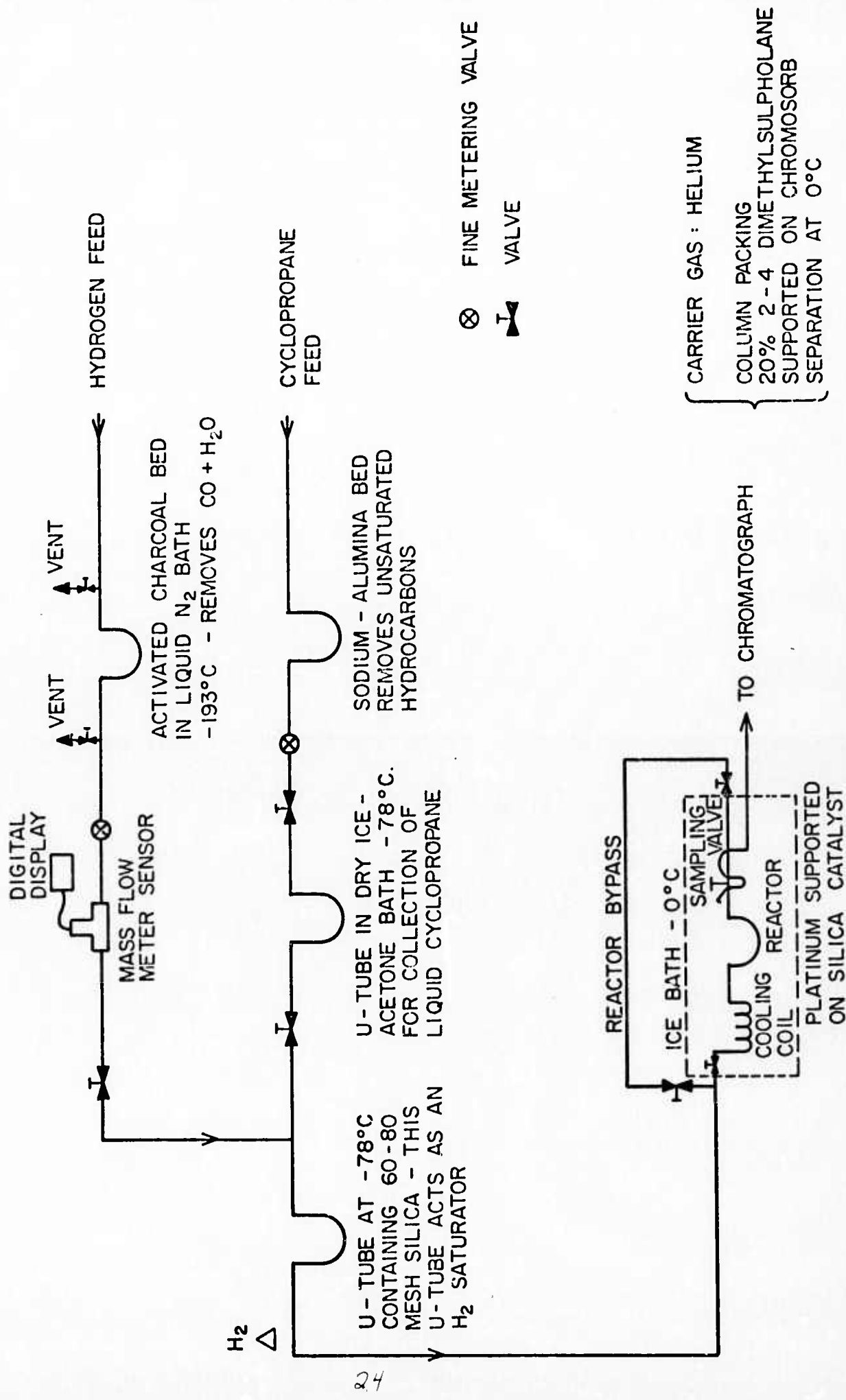
### 3. Catalytic Characterization

The effects of several catalytic reactions on our series of catalysts will be investigated. These reactions will be chosen from among reactions thought to be insensitive to particle size as well as from those thought to be sensitive to particle size. In the latter category we will investigate the isotopic exchange between cyclopentane and deuterium. There is evidence that the isotopic exchange distribution of cyclopentane is sensitive to the size and structure of the metal particles (B1,B2). An apparatus was constructed for the study of this reaction but not operated during the period of this report.

The hydrogenolysis of cyclopropane is probably structure insensitive. A differential flow reactor for the study of this reaction has therefore been designed, constructed and put into operation. This reactor system permits direct determination of catalytic activity for various reactions under conditions of small conversions and in the absence of any physical transport interferences. It will be the basic apparatus used for catalytic activity determinations during the course of this research. A schematic diagram is given in Figure 1.

A complete series of experiments to determine activity for the hydrogenolysis of cyclopropane of one of the catalysts to be studied (1.2% impregnated Pt on 120-140 mesh  $\text{SiO}_2$ , 40.7% dispersion) was conducted during the year. Experimental conditions were varied from -12 to 22°C at approximately one atm. total pressure and a hydrogen to hydrocarbon ratio of 15 to 1. The catalyst activity at each temperature investigated was constant and reproducible within  $\pm 5\%$ . At 0°C, the turnover number (number of reactions per catalytic site per time) determined from these experimental data was  $2.0 \times 10^{-2}$  reactions/site/second. This is to be compared with a value of  $7.1 \times 10^{-2}$  reactions/site/second reported by Boudart et al. (B3) on a much less dispersed (17%) Pt/ $\text{SiO}_2$  catalyst. Activation energy determined in our experiments was  $8.0 \pm \text{ kcal/gmole}$ , which is in good agreement with values

FLOW REACTOR SYSTEM SCHEMATIC FOR MEASUREMENT  
OF RATES OF CYCLOPROPANE HYDROGENOLYSIS



previously determined for Pt/SiO<sub>2</sub> (B4) and Pt on pumice (B5). The apparatus is currently being used to make similar activity measurements for the other three Pt/SiO<sub>2</sub> catalysts in the series, again using the cyclopropane hydrogenolysis reaction.

#### References

- B1. K. Schrage and R. L. Burwell, Jr., J. Amer. Chem. Soc. 88, 4549 (1966).
- B2. J. A. Roth, B. Geller and R. L. Burwell, Jr., J. Res. Inst. Catal. Hokkaido Univ. 16, 221 (1968).
- B3. J. Boudart, et al., J. Catalysis 6, 92 (1966).
- B4. N. A. Dougherty, Ph.D. Thesis, University of California, Berkeley, 1964.
- B5. G. C. Bond and J. Turkevich, Trans. Faraday Soc. 50, 1335 (1954).

#### C. Maximization of Electret Effect in Polyacrylonitrile Films

##### Faculty:

S. H. Carr, Associate Professor, Materials Science

##### Graduate Student:

R. Comstock

The purpose of these experimental investigations has been to show how changes in physical or chemical microstructure can cause changes (maximization) in the magnitude of the permanent electrical polarization. Polyacrylonitrile (PAN) was selected for this research for a number of reasons. 1) Its nitrile chain side groups have an unusually large dipole moment (3.4 D). 2) It is well known to be a good engineering material. 3) Because there is an incomplete understanding of the PAN solid state, studies on the behavior of dipoles within PAN samples should contribute important basic information on this useful material. 4) Finally, pyrolysis treatments are known to cause chemical conjugation of nitrile side groups, and the resulting chemical moieties are predicted to be sites in which electrons or electron holes (as would give rise to a homocharge in polarized solids) could be favorably stabilized.

Experiments were performed in a specially constructed test cell that would permit 1) PAN specimens to be subjected to a variety of annealing, poling and uniaxial stretching sequences and 2) these same specimens to have their thermally stimulated discharge (TSD) currents measured in situ. Temperature stability, both under isothermal and programmed conditions, was accurate to  $\pm 0.01^\circ\text{C}$ ; electrical current noise levels were below  $2 \times 10^{-13}$  amps. Characterization of samples prepared in this apparatus was also done using x-ray diffractometry and optical birefringence measurements.

### 1. Unpolarized PAN

Films in their as-cast condition appear to possess a fairly large level of electrical polarization, as can be inferred from TSD currents measured when heating to  $200^\circ\text{C}$ . A large peak whose maximum is observed at  $180^\circ\text{C}$  can be seen, but the surprising property of this peak is that on re-cycling this same specimen back to  $200^\circ\text{C}$  one sees essentially the same TSD peak. This fact by itself suggests either that there is some chemical or physical source of current other than decaying preferential orientation of dipoles or that dipoles can reorganize into similar anisotropic structures when the solid cools. A comparison of x-ray scattering from PAN in as-cast and annealed states reveals a strong tendency of this material to undergo ordering into a kind of paraerystalline state when heated once. Thus, it is clear that there are strong interchain forces that affect whatever structures exist in this material.

### 2. Polarized PAN

Films of PAN with thicknesses of about 100 microns were given a permanent electrical polarization by heating to  $130^\circ\text{C}$  and subjecting them to fields of  $5 \times 10^5$  V/m with contacting evaporated gold electrodes; the specimens were left at this poling temperature for a minimum of 15 min. prior to cooling to room temperature. Specimens poled thusly were then heated at  $1^\circ\text{C}/\text{min}$ . to  $200^\circ\text{C}$ , and the resulting TSD currents were recorded. Four peaks having maxima at about  $40^\circ\text{C}^{(\delta)}$ ,  $60^\circ\text{C}^{(\gamma)}$ ,  $80^\circ\text{C}^{(\beta)}$  and  $180^\circ\text{C}^{(\alpha)}$  were observed in these data. The first two are weak and have not yet been assigned to a particular mechanism, but the latter two are probably associated with PAN relaxation processes that have already been described in the literature.

Both the 80°C peak and the 180°C peak can be made free of neighboring peaks by "cleaning" (heating to temperatures that discharge all lower temperature peaks but do very little to the peak under investigation). This  $\beta$  process is thought to involve disruption of interchain association in paracrystalline domains, while the  $\alpha$  peak, which also exists in unpolarized PAN, is thought to be due to disruption of interchain association in disordered regions. Activation energies have been computed for both by curve fitting and by Arrhenius plots of  $\ln$  (current) versus  $T^{-1}$ , and the contribution each peak makes to total polarization has been computed in terms of a "normalized polarization." These data are contained in Table C-1. Most interesting is the fact that the  $\alpha$  peak, which is present whether or not the specimens were polarized, exhibits a reversed polarity when the sign of the poling field is appropriately reversed. In other words, if there is an applied field present, even at temperatures below those needed to permit its discharge, the dipolar structure responsible for the  $\alpha$  peak will form with an orientation controlled by the externally applied field rather than by any aspect of the PAN specimen itself.

Films possessing this permanent electrical polarization exhibit a uniform level of birefringence throughout their cross-section but no appreciable change in their x-ray scattering patterns. These facts tend to confirm the proposition that the polarization is a heterocharge originating from oriented dipoles in PAN. Yet, if the dipoles were, in fact, as well oriented as is suggested by the magnitudes of their normalized polarization values, then it is difficult to imagine how the paracrystallinity of these films would also remain unchanged. Intuitively, one expects that such preferred orientation of side groups would lead to smaller interchain distances, to larger deviations in chain packing from a hexagonal symmetry or to some texturization in diffraction effects. Yet, because the present data fail to provide information supporting any such feature, this aspect remains unresolved at the present time.

### 3. Stretched, then Polarized PAN

As can be seen in Table C-1, some improvements in polarization are realized when a film which had previously been heated to 100°C and strained

uniaxially is subjected to the same poling conditions as described above. TSD curves reveal that the  $\gamma$  peak is shifted from 60°C to about 75°C and the  $\beta$  peak is moved to 90°C. The origins of these effects are unknown, but they may reflect improved packing of chains that would, in turn, require slightly higher levels of energy to cause the onset of depolarization. An approximately four-fold increase in normalized polarization due to the relaxation mechanism that produces the  $\alpha$  peak represents a significant, although not spectacular, improvement in PAN electrets. Presumably this benefit is due to the preferred chain orientation that permits better (on average) alignment of their dipolar sidegroups in directions parallel to the poling field. No change in x-ray diffraction and only a slight increase in optical birefringence properties has been observed compared to analogous unpolarized specimens.

#### 4. PAN Simultaneously Stretched and Polarized

Early experiments sought to investigate polarization in films that were simultaneously stretched while the polarizing field was being applied. Because our voltage source was inadequate to create appreciable fields using non-contacting electrodes, this work was suspended. A stronger voltage source is now being procured. The work performed to date indicates that the  $\alpha$  peak is unaffected by poling while stretching but that the  $\beta$  peak increases by a factor of approximately 200. Birefringence was found to increase substantially, suggesting that the origins of the optical anisotropy are appropriately affected by this preparatory treatment. These observations might mean, for example, that an increased mass-fraction of paracrystalline regions results from stretching, and because their formation occurs in the presence of an applied electrical field, the dipoles within them have a strong tendency to become oriented in one direction. It may be that polarization, whose relaxation gives rise to the  $\alpha$  peak, remains unaffected from whatever polarity it had when the film was first solution-cast because the length of time any given part of the film spends between these electrodes is very short (only a few minutes). Much more work needs to be done along these lines.

TABLE C-1  
Data Summary: Permanently Polarized PAN

Depolarization Peak	Specimen Preparation	T <sub>max</sub> , °C	E <sub>act</sub> , Kcal/mole	Normalized Polarization
β	unstretched	80	28	122
β	stretched	90	*	212
α	unstretched	180	45	12,900
α	stretched	180	44	50,600

\*Peak not sufficiently isolated for accurate determination.

D. Mechanical Properties of Composition Modulated Foils

Faculty:

J. E. Hilliard, Professor, Materials Science

Graduate Student:

T. Tsakalakos

Several years ago Professor Hilliard developed a technique for producing thin foils ( $\sim 0.5 \mu\text{m}$ ) containing one-dimensional short wavelength ( $8 - 80 \text{ \AA}$ ) composition modulations. The foils were initially used for an investigation of diffusion over very short distances. However, it later became apparent that they were well suited for studying the effect of structure on properties in general because the structure (in terms of the amplitude and the wavelength of the modulation) was well defined and easily controlled. In a study closely related to the present project, mechanical property tests have been made on Cu-Ni foils containing composition modulations in the range of  $15 - 70 \text{ \AA}$ . These foils exhibited a substantial increase in their elastic modulus as the wavelength of the composition modulation decreased. Under the current program, these studies are to be extended to copper palladium modulated foils with the objective of testing Cahn's theory of strengthening produced by spinodal decomposition. Cahn (D1)

proposed a theory which accounted for the increase in strength of an alloy undergoing spinodal decomposition. Such an alloy has composition fluctuations which can be described by stationary plane waves. These composition fluctuations possess both amplitude and wavelength. When the foils containing such spinodal composition fluctuations are annealed (aged), the wavelengths are affected by the temperature while the amplitude is affected by the annealing time. There is an analogy between the resistance to the passage of a dislocation through a material containing precipitates and the resistance encountered when the dislocation encounters composition gradients and internal stresses caused by spinodal decomposition. Copper and palladium have a large difference in atomic sizes; according to the theory, a composition modulation in this system should produce a very substantial increase in yield strength.

The foils are prepared by evaporating the two components through a rotating pin-wheel shutter. The rotating shutter cuts off the vapor first from one crucible and then from the other, thus building up alternating layers of the two components. Since some diffusion occurs during deposition, the final structure is close to being a sinusoidal function of composition versus distance. The wavelength of the modulation is determined from the location of the sidebands it produces around the Bragg x-ray diffraction peaks.

The mechanical tests are performed in a "bulge" tester that was designed and constructed for this investigation. After the foils are stripped from the substrate, the foil is clamped over a hole (approximately 10 mm in diameter) at the end of a cylinder. Excess gas pressure was applied to the cylinder, and the height of the bulge it produces in the foil is measured with a laser interferometer. Since the excess pressure and the height of the bulge are known, a stress-strain curve can be constructed. There is agreement in the literature on the calculation of the stress in the bulged foil, but various expressions have been given for the strain. The reason for the disagreement is that different approximations have been utilized. In order to resolve this conflict, Professor Hilliard and his students have obtained an exact numerical solution on a computer of the strain distribution

during the period covered by this report. This solution has been used to analyze the data obtained for the Cu-Ni foils (the work on the Cu-Ni foils was supported by Northwestern University).

Several attempts have been made to evaporate the Cu-Pd foils but thus far without success. The problem is that the melting point of the alumina crucibles is too close to that of the Pd, resulting in contamination of the foils. Other crucible materials will be investigated.

Reference

D1. Cahn, Acta Met. 11, 1275 (1963).